Catena 181 (2019) 104098

Contents lists available at ScienceDirect

Catena

journal homepage: www.elsevier.com/locate/catena

Vegetation restoration stimulates soil carbon sequestration and stabilization in a subtropical area of southern China

Xiang Gu[a], Xi Fang[a,b,*], Wenhua Xiang[a,b], Yelin Zeng[a,b], Shiji Zhang[a], Pifeng Lei[a,b], Changhui Peng[b,c], Yakov Kuzyakov[a,d]

[a] Faculty of Life Science and Technology, Central South University of Forestry and Technology, Changsha 410004, China
[b] Huitong National Field Station for Scientific Observation and Research of Chinese Fir Plantation Ecosystem in Hunan Province, Huitong 438107, China
[c] Institute of Environment Sciences, Department of Biological Sciences, University of Quebec at Montreal, Montreal, QC H3C 3P8, Canada
[d] Department of Soil Science of Temperate Ecosystems, Department of Agricultural Soil Science, University of Goettingen, 37077 Göttingen, Germany

ARTICLE INFO

Keywords:
Active carbon pool
Fine root biomass
Resistant carbon pool
Slow carbon pool
Soil organic carbon composition
Vegetation-soil interaction

ABSTRACT

Vegetation restoration affects the stability of soil organic carbon (SOC) by changing the composition of soil carbon pools, including active carbon (C_a), the labile pool of SOC; slow carbon (C_s), the physically stabilized pool of SOC; and resistant carbon (C_r), the chemically stabilized pool of SOC. The aims of this study were to determine how SOC pools changed during restoration of a subtropical forest and to what extent vegetation characteristics and soil properties affected the changes in SOC pools. Soil samples were collected to 40 cm in four plant communities along a restoration chronosequence: scrub-grassland (4–5 years), shrubs (10–12 years), coniferous and broadleaved mixed forest (45–46 years), and evergreen broadleaved forest (90–91 years). Laboratory incubations were used to measure CO_2 production during SOC mineralization, and acid hydrolysis was used to measure C_r. The CO_2 production and C_r data were fitted to a three-component first-order kinetic model to determine the C_a and C_s. Pearson's correlations, stepwise multiple line regressions, and variation partitioning analysis were used to determine the key factors that affected SOC pools. The results showed that vegetation restoration increased the contents of SOC from 1.67 to 47.6 g kg^{-1}, C_a from 0.03 to 0.35 g kg^{-1}, C_s from 1.32 to 24.5 g kg^{-1}, and C_r from 0.33 to 22.8 g kg^{-1}. During vegetation restoration, the increase in SOC was primarily due to carbon (C) stored in stable pools (i.e., C_s or C_r), and the portion of C_r in total SOC increased markedly from 18.5 to 56.3%. Fine root biomass was the primary driver that controlled SOC pools during vegetation restoration. The C/N ratio of litter had a greater effect on C_a and C_s than that of other factors, whereas the soil clay content contributed secondarily to C_r. The results suggest that vegetation restoration increases not only the amounts of SOC, C_a, C_s, and C_r but also the stability of the SOC pool in subtropical soil. The relatively rapid increases in C_s and C_r following vegetation restoration played a crucial role in C sequestration. Therefore, strong measures to preserve natural forests and facilitate vegetation restoration should be the primary approach to increase long-term soil C sequestration in this region.

1. Introduction

The mechanisms of soil organic carbon (SOC) accumulation are uncertain, partly because of the highly complex composition and forms of SOC (von Lützow et al., 2007). SOC is a heterogeneous substance composed of various organic materials that vary in content and stability (Wiesmeier et al., 2014). Based on the decomposition rate and mean residence time (*MRT*), SOC can be partitioned into three pools: active (C_a), slow (C_s), and resistant (C_r) carbon (Tian et al., 2016; Xiao et al., 2016). The C_a is composed of labile carbon (C), such as simple sugars, organic acids, and lipids, and the most readily utilized by soil microorganisms, with an *MRT* of days (Chen et al., 2018; Dikgwatlhe et al., 2014). The C_s consists primarily of physically stabilized C, with an *MRT* of 25–50 years (Cochran et al., 2007). The C_r is stored in the soil as humus and chemically stabilized C and with an *MRT* of 1000–1500 years, is responsible for soil C sequestration and stability (Lian et al., 2018; Liu et al., 2017). Soils with a high proportion of C_r indicate relatively high biochemical stability of SOC and may favor long-term C sequestration (Liu et al., 2017; Wiesmeier et al., 2014). Therefore, to fully understand SOC dynamics and mechanisms of accumulation, the sizes and contributions of the different SOC pools should be determined.

* Corresponding author at: Faculty of Life Science and Technology, Central South University of Forestry and Technology, Changsha 410004, China.
E-mail address: fangxizhang@sina.com (X. Fang).

https://doi.org/10.1016/j.catena.2019.104098
Received 11 December 2018; Received in revised form 21 April 2019; Accepted 29 May 2019
Available online 10 June 2019
0341-8162/

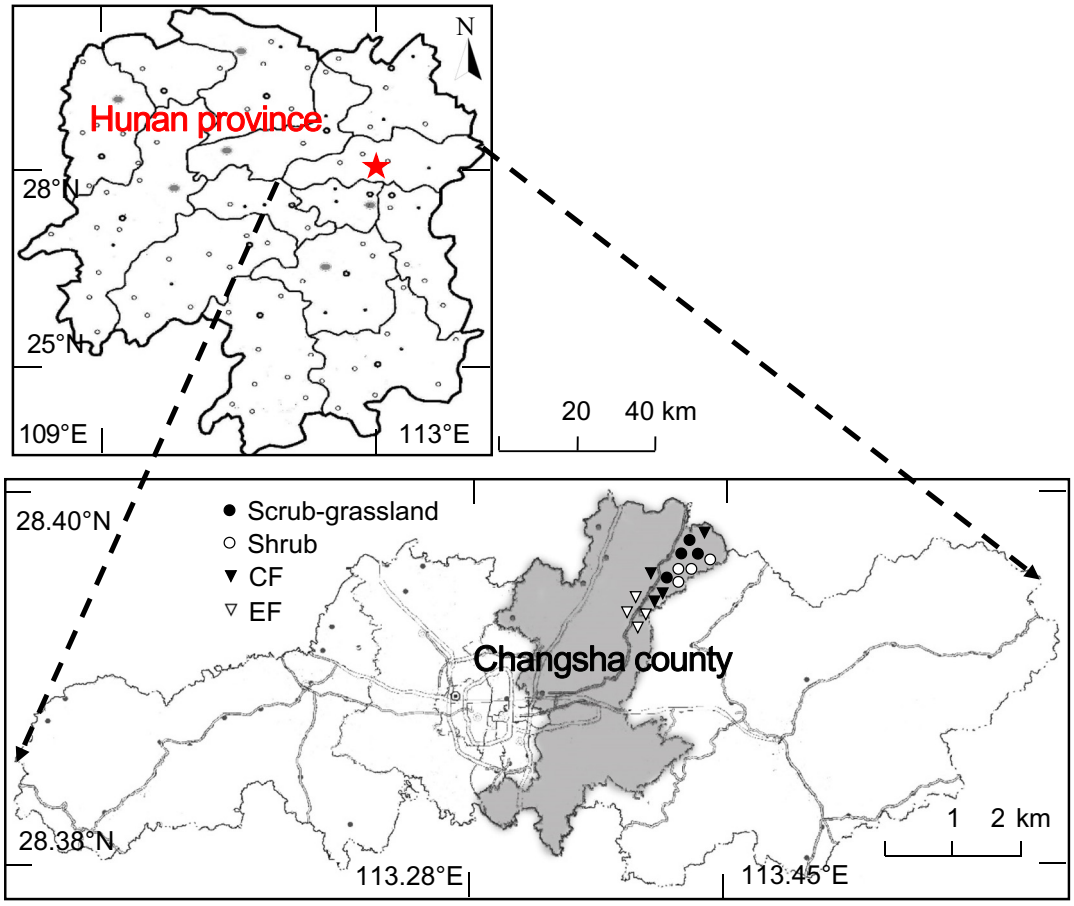

Fig. 1. Location and distribution of the four different vegetation communities. CF is the coniferous and broadleaved mixed forest, and EF is the evergreen broadleaved forest.

Vegetation change is an important factor affecting SOC stocks and accumulation (Ramesh et al., 2015; Wang et al., 2018; Zhao et al., 2015). In vegetation restoration, plant species and community composition change gradually, which may have important impacts on the content and stability of SOC by altering litter quality and quantity (Ramesh et al., 2015), root architecture and exudates (Liu et al., 2014; Zhu et al., 2016), and soil properties (Sá and Lal, 2009; Xie et al., 2013). The changes in SOC during vegetation restoration may not be induced by only one factor but by a variety of factors. Therefore, the SOC can show the following responses to vegetation restoration: (1) continuous increase; (2) no change; (3) decrease; and (4) first decrease and then increase (Powers and Marín-Spiotta, 2017). Numerous studies have focused on the responses of SOC (particularly SOC storage) to land use changes (Francaviglia et al., 2017; Li et al., 2016b) and forest conversions (Chen et al., 2018; Marchand, 2017). By contrast, relatively few studies have investigated the dynamic changes in SOC pools and stability that occur during the succession from a scrub-grassland (an early plant community) that is gradually restored to shrub, secondary forest, and climax forest communities. In addition, the primary factors that control SOC pools during such vegetation restoration have received less attention.

In subtropical areas of China, most climax vegetation (i.e., evergreen broadleaved forests) has been severely degraded or destroyed because of long-term human disturbances and intensive land use activities (Sun et al., 2014; Yang et al., 2009). The Chinese government has pursued forestry ecology projects over the past two decades, promoting the vegetation restoration of subtropical native forests (Xiang et al., 2013). Therefore, a variety of secondary vegetation communities consisting of diverse tree species have formed in subtropical China. Under the specific climatic and soil conditions of subtropical China, a secondary bare area forms after the clearance of a native evergreen broadleaved forest or plantation, and the succession pathway is generally as follows. A scrub-grassland community dominated by herbs and with a few shrubs appears after 2–3 years of natural restoration. After 10 years of natural restoration, a shrub community forms. Then, *Pinus massoniana* Lamb. coniferous forest, *P. massoniana* mixed forest, and deciduous evergreen broadleaved mixed forest gradually form, with the appearance of some light-demanding pioneer trees that include conifer tree species (such as *P. massoniana*) and deciduous broadleaved tree species (such as *Liquidambar formosana*, *Quercus acutissima*, *Choerospondias axillaries*, *Alniphyllum fortunei*). Ultimately, an evergreen broadleaved forest is formed as light-demanding pioneer tree species are gradually replaced by more shade-tolerant tree species, including members of Fagaceae (e.g., *Lithocarpus glaber*, *Cyclobalanopsis glauca*), Theaceae (e.g., *Schima superba*, *Cleyera japonica*), and Polygonaceae (e.g., *Cinnamomum camphora*, *Photinia davidsoniae*, *Litsea coreana*) (Tang et al., 2010a; Xiang and Fang, 2018). Based on the degree of restoration and species composition, these secondary vegetation communities are generally categorized as scrub-grassland, shrub, deciduous broadleaved and mixed deciduous evergreen broadleaved forests, and evergreen broadleaved forests along a restoration gradient (Xiang et al., 2016). Because of the strong changes in aboveground vegetation and soil C stock during this succession (Liu et al., 2015; Zhou et al., 2006), many scientists have focused on the responses of SOC (Chen et al., 2018; Liu et al., 2015; Song et al., 2017) and C_a (Xiao et al., 2016; Yang et al., 2009). However, during vegetation restoration in subtropical China, the variations in SOC pools and the mechanisms of SOC accumulation and stability are not well understood (Liu et al., 2015; Sun et al., 2014).

To estimate the SOC sequestration potential and stability in subtropical China, the changes in SOC pools during vegetation restoration must be quantified and the mechanisms involved identified. To date, the combination of acid hydrolysis, long-term laboratory incubation, and a three-pool first-order kinetics model has been widely and successfully applied to determine different SOC pools and predict SOC dynamics in agriculture (Qian et al., 2013), in forests (Tian et al., 2016; Yang et al., 2007), and under different land uses (Iqbal et al., 2009; Jha et al., 2012). In this study, four distinct vegetation types were selected: scrub-grassland, shrub, coniferous and broadleaved mixed forest (CF), and evergreen broadleaved forest (EF). These vegetation types represent the four main stages during vegetation restoration in the Chinese subtropics. The sizes of SOC pools were measured with a three-pool first-order kinetics model, using the data obtained from laboratory incubations of SOC mineralization and acid hydrolysis analysis. The objective was to test the following two hypotheses: (1) vegetation restoration increases the SOC content and its pool sizes (i.e., C_a, C_r, and C_s), but the increase is greater in C_r and C_s than that in C_a; and (2) vegetation restoration promotes the stability of SOC. In addition, the effects of litter and soil physicochemical properties on SOC pools and stabilization were investigated.

2. Materials and methods

2.1. Study site and plant community description

This research was conducted in Changsha County (28°23′–24′N, 113°17′–27′E), Hunan Province, China (Fig. 1). The climate is humid mid-subtropical monsoon, with an annual average precipitation of 1416.4 mm (primarily between April and August) and an annual mean air temperature of 17.3 °C. Minimum and maximum air temperatures are −10.3 °C in January and 39.8 °C in July and August, respectively. The topography features a typical low hilly landscape, at an altitude of 55–260 m a. s. l. with an average slope of 18–25°. The soils are well-drained clay loam red soil, which originated from slate and shale rock and are classified as Alliti-Udic Ferrosols in the Chinese Soil Taxonomy, corresponding to Acrisol in the World Reference Base for Soil Resource (IUSS Working Group WRB, 2006). Evergreen broadleaf forests are the climax and primary vegetation but have been disturbed by human activities (such as firewood collection) to various degrees. Natural forest protection programs in the past two decades have resulted in a variety of vegetation communities at different stages of restoration in this area.

In October 2015, four vegetation communities with a similar topography (elevation, slope, and aspect) were selected to represent a vegetation restoration gradient (using the method of space-for-time substitution). The communities were the following:

(1) Scrub-grassland (4–5 years): Controlled burns and site preparation were conducted in a native evergreen broadleaved forest in the winter of 1965. *Pinus massoniana* plantations were established in 1966 with no fertilization supplied and were clear-cut in 1990. The woodlands were repeatedly cut until 2012, and the vegetation has naturally recovered. Well-grown herbs and some young shrubs dominated the community at the time of the study, which represented the early stage of restoration in the succession process of the subtropical evergreen broadleaved forest.
(2) Shrub (10–12 years): The native evergreen broadleaved forest underwent a prescribed burn in 1965 and was deforested to establish a *Cunninghamia lanceolata* plantation in 1966, which was clear-cut in 1989. The woodlands were then logged every 3–5 years until 2004. The vegetation naturally recovered to form a shrub community with well-grown shrubs at the time of the study. The shrub community did not have arbor layers and herbaceous plants were relatively infrequent.
(3) Coniferous and broadleaved mixed forest (45–46 years) (CF): The native evergreen broadleaved forest was deforested in the early 1970s and then naturally recovered to a coniferous and broadleaved mixed forest. The communities at the time of the study were approximately 45 to 50 years old and had abundant seedlings and saplings and relatively high plant density. However, the proportion of large-diameter individuals was relatively low.
(4) Evergreen broadleaved forest (90–91 years) (EF): The native evergreen broadleaved forest was well protected against human disturbances and had a relatively stable structure.

In October 2015, plots were randomly established in the different communities: four 20 m × 20 m plots in the scrub-grassland and shrub communities, and four 30 m × 30 m plots in the CF and EF communities (Fig. 1). To investigate the floristic components and tree spatial patterns of the forests, each plot (20 m × 20 m) in the scrub-grassland and shrub communities was subdivided into four subplots (10 m × 10 m), and each plot (30 m × 30 m) in the CF and EF communities was subdivided into nine subplots (10 m × 10 m). Species identity was recorded, and total height, height to the lowest live branch, crown width, and diameter at breast height (DBH) were measured for all individuals with DBH ≥ 1 cm in each plot. The Shannon index (*SI*) was used to quantify the woody plant species diversity of each plant community with formula (1) (Madonsela et al., 2018):

$$SI = -\sum_{i=1}^{S} P_i \ln P_i \quad (1)$$

where S is the total number of species in the community and P_i is the relative frequency of species i in the community. Table 1 summarizes the characteristics and site factors of each community.

2.2. Soil, fine root, and litter sampling

Soil samples were obtained in October 2016. In each permanent plot, three sample points were randomly selected at different slope positions. At each point, the litter was removed and soil samples were collected at depths of 0–10, 10–20, 20–30, and 30–40 cm. Simultaneously, the soil bulk density (BD) of each soil layer was determined using a steel soil core with a 7 cm diameter and 5.2 cm high.

The soil samples from the three points from the same depth within a plot were pooled to form a composite sample. Plant roots, debris, and gravel were removed. A portion of each fresh soil sample was sieved through a 2-mm mesh and kept at 5 °C to measure SOC mineralization. The other portion of each fresh soil sample was air-dried and sieved through a 2-mm mesh for soil particle size fractionation, 1-mm mesh for soil pH, 0.25-mm mesh for SOC and total nitrogen (N), and 0.15-mm mesh for C_r determinations.

A 1 m × 1 m quadrat was set up at the center of each 10 m × 10 m subplot to determine litter biomass (LB). All litter was collected from the ground in these quadrats and transported to the laboratory. The litter was oven-dried at 75 °C to a constant weight, and the dry mass was recorded. The LB of the four vegetation communities is summarized in Table 2. The oven-dried litter was ground and sieved through a 0.25-mm mesh to determine the C and N contents.

The fine root biomass (FB) was obtained using the method suggested by Liu et al. (2014). In brief, roots were sampled at four different points (i.e., east, south, west, and north) from a soil sampling point. At each point, root samples were collected at depths of 0–10, 10–20, 20–30, and 30–40 cm by using a steel auger (10 cm in diameter), placed in plastic bags, and kept at 5 °C. In each permanent plot, 48 root samples were collected, resulting in 192 fine root samples in each plant community. The root samples were soaked in water for 2 h and then swirled in a 0.25-mm mesh to remove the soil and residues affixed to the roots. All roots were divided into two diameter classes (i.e., ≤ 2 mm and > 2 mm), and the fine roots (≤ 2 mm) were oven-dried at 75 °C for 48 h to a constant weight to measure their dry mass. The FB was calculated as follows:

Table 1
Vegetation community characteristics and site factors of the different stages of restoration.

Restoration stage	Dominant plants	Composition (%)	Density of woody plants (individuals ha^{-1})	Shannon index	Average DBH/Ground diameter (cm)	Average tree height (m)	Elevation (m)	Slope aspect	Slope
Scrub-grassland (4–5 years)	*Loropetalum chinense*	34.5	18,130	1.0 ± 0.4a	/	0.9 (0.3–1.8)	120–131	Southeast	18°
	Vaccinium bracteatum	21.6							
	Rhododendron mariesii	12.1							
	Quercus fabri	7.8							
	Castanea mollissima	5.2							
	Others (8 species)	19.0							
Shrub (10–12 years)	*Loropetalum chinense*	17.5	7633	2.0 ± 0.3b	2.7/1.3 (1.0–9.8)/(1.0–1.8)	3.2 (0.8–6.5)	120–135	Northwest	22°
	Cunninghamia lanceolata	14.9							
	Quercus fabri	12.7							
	Vaccinium bracteatum	12.7							
	Litsea cubeba	11.4							
	Others (16 species)	31.0							
Coniferous and broadleaved mixed forest (45–46 years)	*Pinus massoniana*	14.1	17,396	2.2 ± 0.1b	5.7 (1.0–28.0)	6.5 (1.5–20.0)	135–160	Southwest	20°
	Lithocarpus glaber	18.9							
	Loropetalum chinense	14.3							
	Cleyera japonica	11.4							
	Camellia cuspidata	8.9							
	Others (25 species)	32.4							
Evergreen broadleaved forest (90–91 years)	*Lithocarpus glaber*	39.7	20,785	2.1 ± 0.2b	5.6 (1.0–40.0)	5.8 (1.5–20.0)	200–260	Southeast	22°
	Cleyera japonica	14.3							
	Cyclobalanopsis glauca	4.3							
	Cunninghamia lanceolata	4.2							
	Eurya muricata	3.1							
	Others (38 species)	34.4							

The sample size was n = 4 in each plant community. Values are the means for the percent composition, density of woody plants, average DBH, average tree height, elevation, and slope. Values are the mean ± standard deviation for the Shannon index. Values in parentheses are the ranges for diameter at breast height (DBH) or ground diameter and for tree height in each plant community. Different letters indicate differences between restoration stages that are significant at $P < 0.05$.

Table 2
Litter biomass and nutrient characteristics of the four plant communities (stages) during vegetation restoration.

Restoration stage	Litter biomass (kg ha^{-1})	C content in litter layer (g kg^{-1})	N content in litter layer (g kg^{-1})	C/N in litter layer
Scrub-grassland (4–5 years)	1568 ± 928a	315 ± 25.3 ac	9.8 ± 0.3a	35.8 ± 2.6a
Shrub (10–12 years)	6280 ± 851b	277 ± 33.3a	11.2 ± 0.9a	26.0 ± 0.2b
Coniferous and broadleaved mixed forest (45–46 years)	7085 ± 1752b	424 ± 8.6b	11.5 ± 0.5a	38.0 ± 1.6a
Evergreen broadleaved forest (90–91 years)	7795 ± 875b	332 ± 53.9c	14.0 ± 0.2b	23.9 ± 3.5b

Values are the mean ± standard deviation (n = 4). Different letters indicate differences between restoration stages for the same soil layer that are significant at $P < 0.05$.

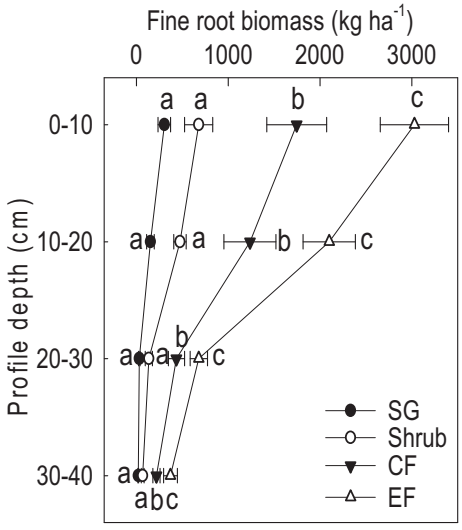

Fig. 2. Fine root biomass by depth (cm) in the four different vegetation communities in subtropical China. SG is the scrub-grassland, CF is the coniferous and broadleaved mixed forest, and EF is the evergreen broadleaved forest. Different letters indicate that the differences between different stages of vegetation restoration are significant at $P < 0.05$. Values are the mean ± standard deviation.

$$\mathrm{FB(kg\ ha^{-1})} = \frac{FBM \times 10^{-1}}{\pi \times (d_s/2)^2} \quad (2)$$

where *FBM* is the fine root dry mass per steel auger and d_s is the inner diameter of the steel auger. The FB of the four vegetation communities is summarized in Fig. 2.

2.3. Chemical analysis

Briefly, the litter C (LC) and N (LN) contents were measured via the $K_2Cr_2O_7$-H_2SO_4 oxidation method and the semimicro-Kjeldahl method, respectively (Tang et al., 2010b). The litter nutrients of the four vegetation communities are summarized in Table 2. Soil pH was analyzed in a soil-to-water (deionized) ratio of 1:2.5 using a pH meter (FE20, Mettler Toledo, Switzerland). Soil total N content was determined using a semimicro-Kjeldahl method (Deng et al., 2013). Clay content (soil particle size fraction < 0.002 mm) was measured by a combined sieve/hydrometer method (Li et al., 2016a). Soil BD was calculated using weights of the dried soil samples and the volume of the steel soil core. The soil physicochemical properties of the four vegetation communities are summarized in Table 3.

SOC contents were determined by the $K_2Cr_2O_7$-H_2SO_4 oxidation method (Deng et al., 2013). The C_r content in soil samples was obtained using the method suggested by Paul et al. (2006). In brief, 1 g of oven-dried, sieved (< 0.15 mm) soil sample was digested with 25 mL of 6 mol L^{-1} HCl at 110 °C for 18 h. After cooling, the digested soil samples were washed with deionized water to remove excess Cl^-, dried at 60 °C, and measured by the $K_2Cr_2O_7$-H_2SO_4 oxidation method.

2.4. Laboratory incubation

Long-term laboratory incubations, which measure CO_2 emissions from SOC mineralization, offer a biological approach to differentiate C_a and C_s pools, whereby the C_a pool is rapidly mineralized by soil enzymes and microbes and the subsequent C_s pool is more slowly mineralized (Cochran et al., 2007; Iqbal et al., 2009; Qian et al., 2013). SOC mineralization was determined by the laboratory incubation method (Paul et al., 1999): a 50 g sample of fresh soil was incubated in a 500 mL conical flask at 35 °C for 94 days. During the incubation, the soil moisture was maintained at 60% water-holding capacity by adding distilled water, to simulate the average field moisture condition. A vial containing 10 mL of 0.2 mol L^{-1} NaOH was placed in each flask, and the flasks were sealed with rubber stoppers and placed in an incubator. For each soil sample, 2 replicates were incubated together. The same vials were removed over 3, 6, 9, 13, 17, 21, 28, 35, 42, 49, 64, 79, and 94 days after initiating the incubation and titrated with 0.1 mol L^{-1} potassium acid phthalate ($C_8H_5KO_4$), after first adding 3 mL of 1.5 mol L^{-1} $BaCl_2$ with phenolphthalein as an indicator. The amount of *CO_2-C* evolved was calculated as follows:

$$CO_2 - C\,(\mathrm{g\ kg} - 1) = \frac{6 \times c(V_0 - V_1)}{W \times k} \quad (3)$$

where V_0 and V_1 are the respective volumes of $C_8H_5KO_4$ consumed for titrating NaOH in the control and amended soil samples (mL); c is the normality of $C_8H_5KO_4$ (mol L^{-1}); W is the weight of the fresh soil sample (g); and k is the coefficient for the conversion of fresh soil to dried soil.

However, laboratory incubations alone are insufficient for determining the size and turnover rate of the C_r pool (Paul et al., 2006). To obtain information on the C_r pool, the most common chemical method is an acid hydrolysis using 6 mol L^{-1} HCl; the hydrolysable fraction represents the C_r pool (Lian et al., 2018; Rovira and Vallejo, 2007). Modeling SOC dynamics is also an effective tool for predicting and distinguishing the various C pools (Smith et al., 2012): a three-pool first-order kinetics model can accurately predict dynamic changes in the SOC pool (Yang et al., 2007). Paul et al. (1999) successfully defined C_a, C_s, and C_r pool sizes and SOC dynamics by using a combined method involving long-term laboratory incubation of soils and CO_2 measurements, acid hydrolysis, and a three-pool first-order kinetics model. Others have coupled lab incubations with an acid hydrolysis (Fortuna et al., 2003; Paul et al., 2001), but Paul et al. (2006) provide convincing evidence that such an approach is more useful for determining SOC pools than other methods (e.g., ^{13}C, ^{14}C, and DAYCENT model).

SOC pools are generally divided into C_a, C_s, and C_r pools according to the decomposition rate and turnover time of SOC. The size and kinetics of these SOC pools were determined using the *CO_2-C* evolved from SOC mineralization during the 94-d laboratory incubation. Each pool size was estimated by curve-fitting the *CO_2-C* evolved per unit of time using a three-component first-order kinetic model (Jha et al., 2012):

$$C_{SOC} = C_a e^{-k_a t} + C_s e^{-k_s t} + C_r e^{-k_r t} \quad (4)$$

where C_{SOC} is the total SOC at time t (days); C_a, C_s, and C_r are the size of active, slow, and resistant carbon pools (g kg^{-1}), respectively; k_a, k_s,

Table 3
Soil physicochemical properties of the four plant communities (stages) during vegetation restoration.

Restoration stage	Soil depth (cm)	Soil texture	pH	C/N	Bulk density (g cm^{-3})	Clay content (soil particle size fraction < 0.002 mm)
Scrub-grassland (4–5 years)	0–10	Silty loam soil	4.4 ± 0.1a	18.1 ± 1.2ab	1.4 ± 0.2a	15.6 ± 2.9ab
	10–20	Silty loam soil	4.7 ± 0.1a	15.6 ± 5.4a	1.5 ± 0.1a	11.4 ± 2.0a
	20–30	Silty loam soil	4.8 ± 0.1a	16.1 ± 2.5a	1.5 ± 0.1a	10.2 ± 2.2a
	30–40	Silty loam soil	5.1 ± 0.1a	13.1 ± 4.4a	1.5 ± 0.1a	8.7 ± 2.4a
Shrub (10–12 years)	0–10	Silty loam soil	4.7 ± 0.1b	15.3 ± 2.2a	1.4 ± 0.1a	11.2 ± 2.2a
	10–20	Silty loam soil	4.9 ± 0.1a	14.4 ± 1.6a	1.6 ± 0.0a	17.2 ± 3.6b
	20–30	Silty loam soil	5.0 ± 0.2a	13.9 ± 3.4a	1.6 ± 0.0a	12.4 ± 2.8b
	30–40	Silty loam soil	5.1 ± 0.2a	10.4 ± 2.4a	1.7 ± 0.0a	11.2 ± 2.4b
Coniferous and broadleaved mixed forest (45–46 years)	0–10	Clay loam	4.2 ± 0.2 ac	18.4 ± 1.5b	1.2 ± 0.3a	16.5 ± 7.3ab
	10–20	Silty loam soil	4.4 ± 0.1b	16.7 ± 0.4a	1.4 ± 0.2a	14.7 ± 7.1b
	20–30	Silty loam soil	4.4 ± 0.1b	14.5 ± 1.6a	1.5 ± 0.2a	12.9 ± 1.7b
	30–40	Silty loam soil	4.5 ± 0.1b	12.3 ± 1.4a	1.5 ± 0.1a	10.0 ± 1.3b
Evergreen broadleaved forest (90–91 years)	0–10	Clay loam	4.0 ± 0.1c	15.6 ± 1.7ab	1.3 ± 0.1a	19.7 ± 3.6b
	10–20	Clay loam	4.3 ± 0.1b	13.6 ± 0.7a	1.4 ± 0.0a	18.1 ± 6.0b
	20–30	Clay loam	4.3 ± 0.1b	12.3 ± 1.3a	1.5 ± 0.0a	14.9 ± 5.5b
	30–40	Clay loam	4.3 ± 0.3b	11.9 ± 1.3a	1.5 ± 0.1a	12.3 ± 3.8b

Values are the mean ± standard deviation (n=4). Different letters indicate differences between restoration stages for the same soil layer that are significant at $P < 0.05$.

and k_r are the pool decay constants (day^{-1}), respectively; and k is the reciprocal of mean residence time (MRT^{-1}).

The turnover time of each pool is influenced by differences in temperatures between the laboratory and field. Because C_r typically has a low turnover rate, the *MRT* in the field (MRT_{field}) of C_r was assumed to be 1000 years, which would have little influence on the other two pools (C_a and C_s) and the model simulations. The laboratory *MRT* (MRT_{lab}) of C_r derived from the laboratory incubation was scaled to the average annual temperature at the study site (*MAT*, °C) by using the temperature coefficient (Q_{10}) and the MRT_{field} as follow:

$$Q_{10} = 2^{\left(\frac{25-MAT}{10}\right)} \quad (4)$$

$$MRT_{lab} = \frac{MRT_{field}}{Q_{10}} \quad (5)$$

where *MAT* is 17 °C for the study site. The three parameters (k_a, k_s, and C_a) were estimated by nonlinear regression. The C_s was defined as $C_s = C_{SOC} - C_a - C_r$.

2.5. Statistical analyses

The sizes of each C pool were fitted to the kinetics model by using a nonlinear regression procedure. The differences in aboveground vegetation factors (*SI*, FB, LB, LC, LN, and the C/N ratio of litter (LC/LN)), soil properties (C/N, pH, BD, and clay content), the daily amount of SOC mineralization, and the size of SOC pools among the four restoration stages or soil layers were tested using one-way ANOVA with the least significant difference (LSD) test. $P < 0.05$ was considered statistically significant.

Pearson correlations were used to examine the relationships among SOC pools and soil factors (C/N, pH, BD, and clay content) and vegetation factors (*SI*, FB, LB, LC, LN, and LC/LN). Stepwise multiple linear regressions were performed to select those factors that significantly affected the SOC pools. Furthermore, to understand the joint and independent contributions of these two categories (vegetation and soil factors) to SOC and its pools, a variation partitioning analysis (VPA) was performed using the R package 'vegan' v2.3–3. Before the VPA was set up, the variance inflation factor (VIF) was calculated to select suitably independent variables using the R package 'car' 2.1-2. The criterion of VIF < 3 was used to remove those variables with strong multicollinearity (Yang et al., 2017). All statistical analyses were performed using R version 3.1.2 software (R Core Team, 2015).

3. Results

3.1. SOC mineralization in the four vegetation communities

The daily amount of SOC mineralization in the different stages of vegetation restoration is shown in Fig. 3. The daily amount of SOC mineralization reached a peak on the third day of the incubation, rapidly declined between day 3 and 17, and then tended to stabilize after 17 days.

The daily amount of SOC mineralization varied with vegetation stage and was significantly higher in the EF than that in the scrub-grassland, shrub, and CF. However, the differences in the daily amount of mineralization among the four restoration stages tended to decrease with the increase in soil depth. Generally, the daily SOC amount of mineralization declined with increasing soil depth in all vegetation types (Fig. 3).

3.2. Contents of SOC, C_a, C_s, and C_r in the four vegetation communities

The restoration of vegetation markedly increased the content of SOC and its pools (Fig. 4). The highest and lowest SOC contents were recorded in the EF (47.6 g kg^{-1}) and scrub-grassland (1.67 g kg^{-1}), respectively. The SOC content in the EF was 3.89 to 9.87-fold higher than

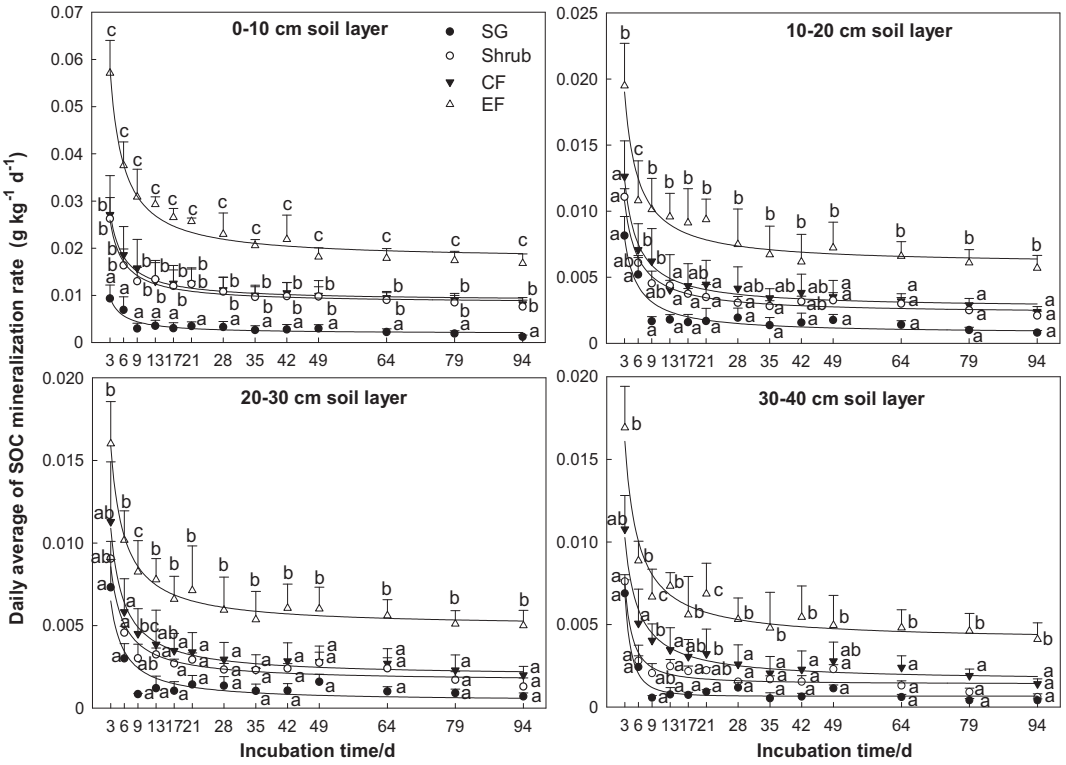

Fig. 3. Daily average amounts of SOC mineralization at four different depths (cm) in the four vegetation communities in subtropical China. SG is the scrub-grassland, CF is the coniferous and broadleaved mixed forest, and EF is the evergreen broadleaved forest. Different letters indicate significant differences between restoration stages for the same soil layer ($P < 0.05$). Values are the mean ± standard deviation (n = 4).

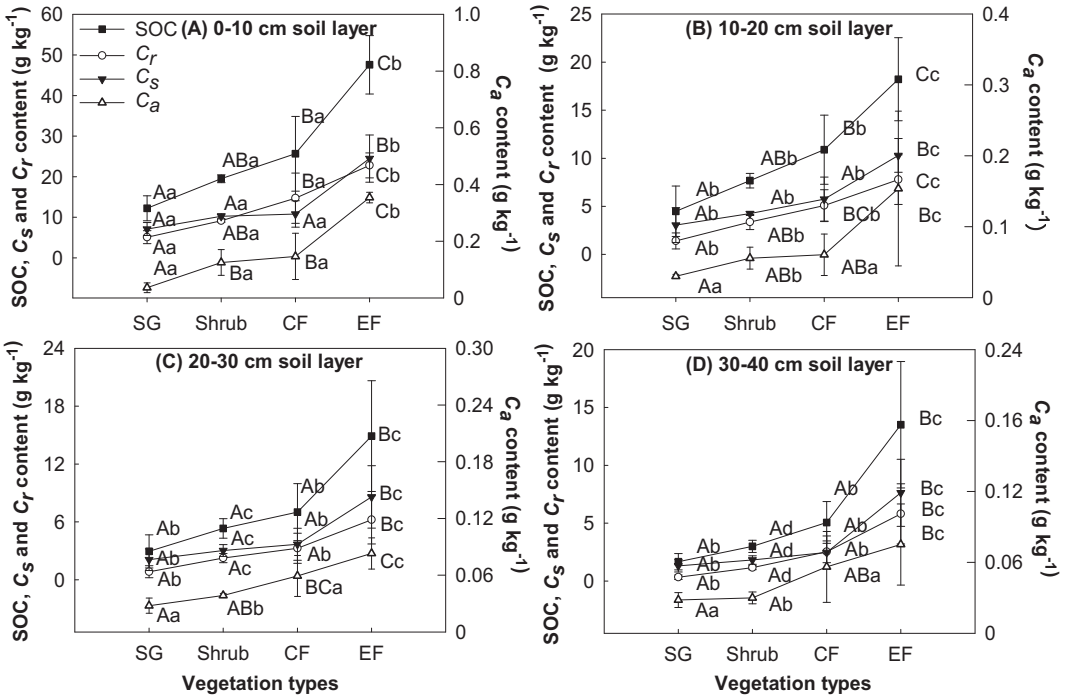

Fig. 4. The contents of SOC and its pools at four different depths (cm) in the four vegetation communities in subtropical China. SG is the scrub-grassland, CF is the coniferous and broadleaved mixed forest, and EF is the evergreen broadleaved forest. Different capital letters indicate differences between restoration stages that are significant at $P < 0.05$, whereas different lowercase letters indicate differences between soil layers within the same restoration stage that are significant at $P < 0.05$. Values are the mean ± standard deviation (n = 4).

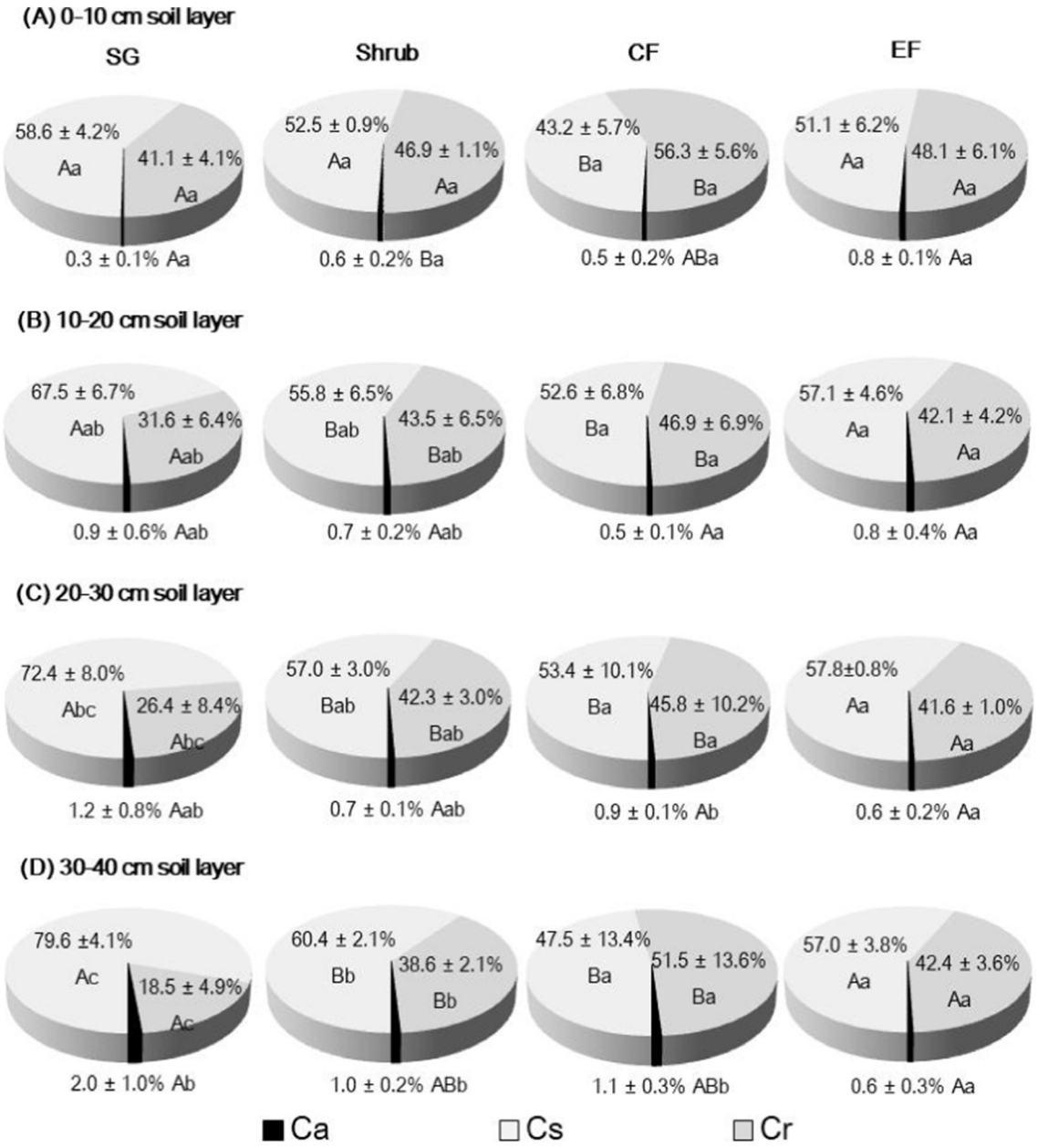

Fig. 5. The contributions (%) of active carbon (C_a), slow carbon (C_s), and resistant carbon (C_r) to SOC at four different depths (cm) in the different vegetation communities in subtropical China. SG is the scrub-grassland, CF is the coniferous and broadleaved mixed forest, and EF is the evergreen broadleaved forest. Different capital letters indicate differences between restoration stages that are significant at $P < 0.05$, whereas different lowercase letters indicate differences between soil layers within the same restoration stage that are significant at $P < 0.05$. Values are the mean ± standard deviation (n = 4).

that in the scrub-grassland. Significant differences in SOC pools among the four vegetation types were also detected at all soil depths. For the 0–10 cm depth, the C_a content in the EF exceeded that in the scrub-grassland, shrub, and CF by 0.32, 0.23, and 0.21 g kg^{-1}, respectively. However, no differences in C_a content were detected between the EF and the CF in the other three soil layers. The C_a content in the EF was 2.68 to 9.78-fold higher than that in the scrub-grassland. The highest C_s content was in the EF, which was 13.7–17.4, 4.54–7.24, 4.91–6.51, and 5.15–6.31 g kg^{-1} higher than that in the other vegetation types at 0–10, 10–20, 20–30, and 30–40 cm depths, respectively. The C_s content in the EF was 3.37 to 5.78-fold higher than that in the scrub-grassland. The highest C_r content was in the EF, which was 8.07–17.7, 2.70–6.37, 2.94–5.38, and 3.27–5.48 g kg^{-1} higher than that in the other vegetation types at 0–10, 10–20, 20–30, and 30–40 cm depths, respectively. The C_r content in the EF was 4.48 to 17.8-fold higher than that in the scrub-grassland.

The contents of SOC and its pools all decreased with soil depth (Fig. 4). In the four restoration stages, the contents of SOC and its pools were significantly higher in the 0–10 cm layer than those in the other soil layers ($P < 0.05$), except for the C_a content in the scrub-grassland and CF.

3.3. Contributions of C_a, C_s, and C_r to SOC in the four vegetation communities

Over the course of restoration, the C_a contributed only 0.3–2.0% to the SOC (Fig. 5). The C_a/SOC ratio in the 0–10 cm soil layer increased with restoration, but the ratio decreased in the deeper soil layers. The C_s/SOC ratio declined markedly from 58.6 to 79.6% in the scrub-grassland to 43.2–53.4% in the CF and then increased slightly to

Table 4
Pearson correlation coefficients between the contents of SOC pools and soil physicochemical properties and vegetation features for the entire study area.

Items	Soil				Vegetation					
	C/N	pH	BD	Clay	*SI*	FB	LB	LC	LN	LC/LN
SOC	−0.134	−0.790**	−0.397	0.751**	0.590*	0.879**	0.761**	−0.201	0.884**	−0.613*
C_a	−0.262	−0.759**	−0.420	0.759**	0.612*	0.907**	0.762**	−0.186	0.935**	−0.619*
C_s	−0.135	−0.756**	−0.376	0.697**	0.552	0.833**	0.621*	−0.308	0.864**	−0.621*
C_r	−0.126	−0.801**	−0.406	0.785**	0.610*	0.900**	0.824**	−0.077	0.877**	−0.489

C_a is active carbon, C_s is slow carbon, C_r is resistant carbon, BD is bulk density, *SI* is the Shannon index, FB is fine root biomass, LB is floor litter biomass, LC is the organic carbon content in litter, LN is the nitrogen content in litter, LC/LN is the ratio of C to N in litter. The sample size was n = 16.

* Significant at $P < 0.05$.

** Significant at $P < 0.01$.

51.1–57.8% in the EF (Fig. 5). The C_r/SOC ratio ranged from 18.5 to 41.1% in the scrub-grassland, increased to 46.9–56.3% in the CF, but then slightly decreased to 41.6–48.1% in the EF.

The ratios of C_a, C_s, and C_r to SOC also varied significantly with soil depth. The C_a/SOC ratio in the scrub-grassland, shrub, and CF communities increased with depth, whereas the ratio in the EF decreased. In the scrub-grassland and shrub community stages, the C_s/SOC ratio increased and the C_r/SOC ratio decreased with depth, but in the CF and EF, the same trends were observed in the top three layers (Fig. 5).

3.4. Factors influencing the SOC and its pools

The contents of SOC pools were significantly positively correlated with soil clay content, *SI* (except C_s), LB, LN, and FB ($P < 0.01$) and with the ratio LC/LN ($P < 0.05$), but the pool contents were significantly negatively correlated with soil pH ($P < 0.01$). No significant associations were detected between SOC pool contents and BD, soil C/N ratio, or LC. Notably, the contents of the SOC pools were more strongly associated with FB ($r = 0.833$–0.907, $P < 0.01$) and LN ($r = 0.864$–0.935, $P < 0.01$) than with any other factors (Table 4).

Stepwise regression showed that FB and the LC/LN ratio together explained 91.6% of the variation in C_a, of which FB explained 80.7% and the LC/LN ratio explained 10.9%. Together, FB, LC/LN ratio, and soil pH explained 90.4% of the variation in C_s, of which FB explained 66.7% and the LC/LN ratio explained 14.7%. Together, FB and soil clay content explained 85.0% of the variation in C_r, of which FB explained 79.2% (Table 5).

Furthermore, the VPA revealed that the combination of vegetation and soil factors of the four communities explained 94, 97, 96, and 88% of the variation occurring in the SOC, C_a, C_s, and C_r, respectively (Fig. 6). Whereas the vegetation factors alone explained 6–35% of this variation, and the soil factors alone explained much less (4–15%), their interaction explained 46–78% of the variation in SOC, C_a, C_s, and C_r during the restoration process.

Table 5
Stepwise multiple linear regressions for active carbon (C_a), slow carbon (C_s), and resistant carbon (C_r) using belowground soil and aboveground vegetation predictors during vegetation restoration.

$P < 0.001$ indicates that the final regression model was highly significant; the sample size was $n = 16$.

Response variable	Predictor	Adjusted R^2	*F*	*P*
C_a	FB	0.807	51.2	< 0.001
	FB, LC/LN	0.916	66.1	< 0.001
C_s	FB	0.667	25.0	< 0.001
	FB, LC/LN	0.814	27.3	< 0.001
	FB, LC/LN, pH	0.904	38.8	< 0.001
C_r	FB	0.792	46.8	< 0.001
	FB, Clay	0.850	35.0	< 0.001

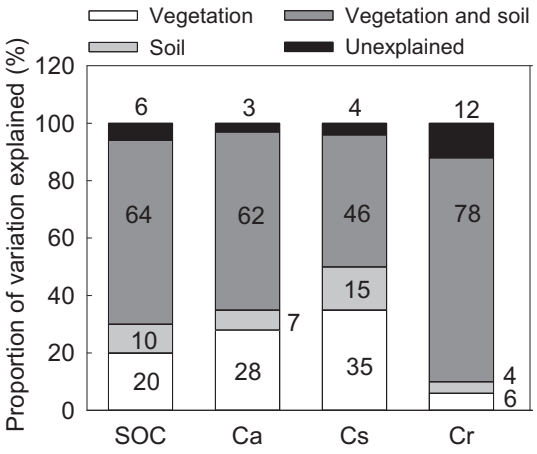

Fig. 6. The contributions of vegetation and soil factors to the proportion of variation explained (%) in the contents of soil organic carbon (SOC), active carbon (C_a), slow carbon (C_s), and resistant carbon (C_r). The numbers embedded in each bar stand for the percentage of variation in SOC or SOC pools that can be explained by the corresponding factor; The unexplained portion (black) is the percentage of variation not explained by either factor; the vegetation and soil portion (dark gray) is the variation explained by an interactive effect of vegetation and soil factors; the soil portion (light gray) is the percentage of variation explained by soil factors alone; the vegetation portion (white) is the percentage of variation explained by vegetation factors alone.

4. Discussion

4.1. Changes in SOC sequestration and stabilization during vegetation restoration

In this study, the contents of SOC and its pools increased along the vegetation restoration gradient, particularly under the conversion from scrub-grassland to EF in the 0–10 cm layer. These results suggest that soil acted as a C sink during vegetation restoration. Similarly, in the conversion of grassland to primary forest, the contents of SOC increased from 29.1 to 73.9 g kg^{-1} (Liu et al., 2015), and the natural restoration of vegetation from pioneer weeds to climax forest caused increases in contents of SOC and labile and nonlabile SOC (Zhao et al., 2015). The conversion of grassland to a 34-year-old plantation and forest not only developed the SOC stock but also increased the contents of active and resistant C (Nath et al., 2018). Crow et al. (2009) suggest that as SOC increases, it is primarily stored in the C_r pool, whereas the C_a pool tends to remain small. In this study, the increment also varied for different SOC pools during vegetation restoration. Across all restoration stages, the smallest increment was in the C_a pool (0.02–0.32 g kg^{-1}), compared with the larger increments in the C_s (4.54–17.4 g kg^{-1}) and C_r (2.70–17.7 g kg^{-1}) pools. Thus, during the vegetation restoration, the increase in SOC was primarily stored in the more stable C pools (i.e., C_s and C_r), which should contribute to C stabilization. These results

support the first hypothesis of this study and further demonstrate that the recovery of vegetation in this area could increase the amount of stable SOC and benefit the sequestration of C in soils.

Among the SOC pools, the C_a is primarily from labile organic materials of plant residues and roots (Liu et al., 2017), which are easily utilized by soil microbes and contribute greatly to SOC mineralization (Jha et al., 2012). The relatively slow accumulation of C_a may be because the SOC mineralization rate increased significantly during the restoration process (Fig. 3). By contrast, C_r and C_s are composed of relatively stable C, which is more difficult to decompose by soil-dwelling microorganisms, and have *MRTs* of > 10 years, reaching even thousands of years (Wiesmeier et al., 2014; Zhang and Zhou, 2018). Owing to their slow turnover rates, C_r and C_s tend to accumulate more in soil as vegetation is restored (von Lützow et al., 2007). Another possible explanation is that inter-conversions may occur among C_a, C_r, and C_s. Vegetation changes following land use change not only influence the contents of active organic C and SOC by changing the inputs of organic matter to soil but also induce the conversion between active organic C and nonactive C in SOC by affecting the physical protection provided by soil aggregates (An et al., 2010; Hyvönen et al., 2007; Pandey et al., 2014). Thus, based on the present study, vegetation restoration led to increases in the contents of SOC and C_a, which further induced the inter-conversions between C_a and C_s and C_r. In addition, during vegetation restoration, an increase in plant litter inputs to soil can generate positive priming effects (Crow et al., 2009; Schimel and Weintraub, 2003), which may accelerate the movement of C inputs to soil into stable fractions of SOC (Hyvönen et al., 2007).

Some consider the C_r portion to be an indicator of the biochemical quality and stability of SOC (Rovira and Vallejo, 2007). Generally, when the C_r portion is high, the biochemical quality of SOC is low, and the SOC pool is more stable (Nath et al., 2018; Zhang et al., 2009). Liu et al. (2017) reported that the contribution of C_r to SOC increased from 49.4 to 66.3% following agricultural land use change from pasture to cropland. The C_r/SOC ratio in woodland (73.9%) was greater than that in paddy (45.2%), orchard (59.1%), and upland sites (36.5%; Iqbal et al., 2009). In the current study, the results are consistent with those of the above studies and showed that the C_r/SOC ratio tended to increase with vegetation restoration (Fig. 5). Therefore, the increase in the ratio could be interpreted as support for the second hypothesis that vegetation restoration would increase the stability of the SOC pool. However, the highest C_r/SOC ratio was detected in the CF rather than in the EF, which was most likely because the litter of the CF contained more lignin and other recalcitrant compounds than broadleaf litter, leading to high inputs of chemically recalcitrant material to the soil (Crow et al., 2009).

In the four vegetation communities spanning the main stages of restoration in this study, the contents of SOC and its pools primarily accumulated in the top soil layer and decreased with an increase in soil depth (Fig. 4). These results are consistent with those of Chabbi et al. (2009), who found that the contents of SOC and its pools decreased with soil depth. The authors suggested that the decrease with depth was related to decreases in organic C inputs from litter and root material. Plant litter, root exudates, and fine root turnover are the primary sources of SOC (Zhao et al., 2015). The abundant inputs of plant litter and fine roots to the topsoil, coupled with a lack of fresh plant residue inputs in deeper soil layers (Li et al., 2017; Sun et al., 2014), should lead to higher contents of SOC, C_a, C_s, and C_r and faster increases in SOC and its pools in the topsoil horizon than their corresponding dynamics in deeper soil layers. Because plant litter and fine root inputs decline with increasing soil depth, the soil microbial biomass is notably reduced in subsoil compared with that found in topsoil. This explanation is the most plausible for the declining contents and increasing rates of SOC and its pools when going down the soil profile (Chabbi et al., 2009). Furthermore, although the input of residues and materials from plant photosynthesis to the soil at depth may be reduced, plants consume more nutrients from the soil at increasing depths (Barreto et al., 2011; Sun et al., 2014). This indirect effect of plant growth is most likely an important factor that controls the contents and increases in SOC, C_a, C_s, and C_r during the course of vegetation restoration.

4.2. Key factors affecting SOC and its C_a, C_s, and C_r pools

In the subtropical study area, the climate is similar among the four vegetation communities examined. Therefore, vegetation restoration facilitated the SOC accumulation and stabilization by altering vegetation factors (such as biomass input and litter properties) and soil factors (such as soil physicochemical properties) (Deng et al., 2016; Li et al., 2016a).

Because the ultimate source of SOC is CO_2 fixed by plants (Russell et al., 2004), the amount and chemical composition of fresh organic materials derived from litter and roots directly contribute to the content and composition of SOC (García-Díaz et al., 2018; Song et al., 2017). Vegetation types and properties can influence the level and stability of SOC via the input of vegetation biomass in plant litter and roots (Li et al., 2016a; Li et al., 2017; Yu et al., 2017). Litter quality is a key factor that controls nutrient release from litter and formation and accumulation of C in soil during the progress of vegetation restoration (Liu et al., 2015; Wang et al., 2016). In this study, vegetation factors explained 6–35% of the variation in content of SOC and its pools (Fig. 6). As vegetation restoration advanced, the *SI*, LB, and FB increased, and the quality of the litter layer improved significantly. The EF had the highest *SI*, LB, FB, and litter quality, compared with the other three vegetation community types (Tables 1 and 2, Fig. 2). The contents of SOC and its pools were significantly correlated with vegetation factors, i.e., the *SI*, FB, LB, LN, and the LC/LN ratio (Table 4), demonstrating that both plant biomass input and substrate quality are most likely important regulators of C sequestration and stabilization in soils.

The study also revealed that soil factors explained 4–15% of the variation in content of SOC and its pools. This result provided evidence for the close relationships between soil factors and SOC content and stabilization. These relationships are close because the content of SOC is determined by the supply of biologically available substrate, and soil factors significantly affect a range of properties associated with the soil microbial community and its ability to process C (Kemmitt et al., 2006). The SOC pools are closely related to a wide range of soil chemical and physical properties (Deng et al., 2016; Sá and Lal, 2009). Soil N and P are essential for the biochemical stabilization of C in soils, which protects soil organic matter with humus from further decomposition (Kirkby et al., 2011). A high content of clay particles in soil tends to increase the storage of SOC by physically protecting SOC from decomposition (Li et al., 2016a) and chemically protecting SOC by the sorption and complexation of organic molecules (Ajami et al., 2016; West and Six, 2007). In addition, soil clay particles facilitate organo-mineral complexes, which stabilize SOC (Six et al., 2002). A decrease in soil pH may result in increases in SOC contents in forests by affecting the conditions for microbial growth (Chen et al., 2004). The findings of the current study extend the previous general results and show that the clay content increased as restoration proceeded through the four community stages, but the soil pH value decreased (Table 3). Soil clay content and pH were significantly associated with the content of SOC and its pools. However, strong relationships between SOC, C_a, C_s, and C_r and the soil C/N ratio under vegetation recovery were not revealed (Table 4), illustrating that the total amount of nutrients in the soil rather than the soil quality was the primary factor regulating the contents and distributions of SOC in the study region.

This study also found that vegetation and soil factors did not act alone but rather their interactions drove the changes observed in contents of SOC and its pools during vegetation restoration. Hence, to better understand the distribution and dynamics of SOC pools, the interactions between vegetation and soil require careful investigation. Based on these results, SOC pool contents and stabilization mechanisms

were apparently influenced by litter and soil physicochemical properties.

Although both vegetation and soil factors influenced the content of SOC and its pools, their ability to explain the variation in C_a, C_s, and C_r differed. The FB played the dominant role in influencing C_a, C_s, and C_r during vegetation restoration. This dominant contribution by FB to C dynamics under forest restoration may be explained by the role that plant roots have generally in the input and output of SOC (Richter et al., 1999; Zhu et al., 2017). Although both plant litter and roots are main sources of C inputs to soil, the contribution of root biomass particularly that of FB, is considered as paramount (Arthur and Fahey, 1992; Robertson and Alongi, 2016). The organic matter input into soil via roots can be more than twice that from plant litter (Arthur and Fahey, 1992). Compared with roots, plant litter has a limited influence on SOC (Rasse et al., 2005). In addition, plant roots can modify soil properties and affect the soil microenvironment, which can alter SOC decomposition and stabilization (Rosell et al., 2000). Thus, the results of this study reinforce that augmentation of FB can improve the contents of SOC pools. Apart from FB, the C/N ratio of litter was an important determinant of C_a and C_s during vegetation restoration. This result implies that litter quality rather than litter biomass played a more important role in SOC accumulation. Soil clay was regarded as a secondary dominant indicator of C_r, supporting the findings of Liu et al. (2015) and Qian et al. (2013) that clay content appears to be crucial for the capacity of a soil to stabilize SOC. Therefore, this study provided evidence that the content and stability of SOC pools were controlled by different factors.

5. Conclusions

The vegetation restoration increased the contents of SOC and its pools in four soil layers. In the EF, the contents of SOC, C_a, C_s, and C_r were 3.89 to 8.07, 2.68 to 9.78, 3.37 to 5.78, and 4.48 to 17.8-fold greater, respectively, than those of the scrub-grassland. The increase in SOC during vegetation restoration was primarily stored as C_s and C_r, which contribute to SOC accumulation and stabilization. The contents of SOC and its pools in the four stages of restoration primarily accumulated in the top soil layer and decreased in deeper soil layers. Litter biomass, nitrogen and carbon content in litter, fine root biomass, Shannon index, and soil clay content were all correlated with the content of SOC and its pools. Notably, among these factors, fine root biomass contributed the most to the variation in content of SOC and its pools. However, the controlling factors differed for the different SOC pools. The ratio of C to N in litter was an important controlling factor for C_a and C_s, whereas soil clay content only played an important role for C_r. Soil pH was only an important controlling factor for C_s. The synergistic interaction between vegetation and soil factors was the primary driver of the changes in contents of SOC and its pools during vegetation restoration in this subtropical area of China. Thus, strong measures taken to preserve natural forests and to facilitate the restoration of vegetation would be the main approach to increase long-term soil C sequestration in this region.

Declaration of Competing Interest

Declarations of interest: none.

Acknowledgements

This work was supported by the National Forestry Public Welfare Industry Research Project (grant no. 201504411). We would like to thank the following postgraduates for their assistance in our field investigations and laboratory analyses: Leida Li, Zhaodan Liu, Jinlei Chen, Liufang Wang, and Shangyi Li. We are also grateful to the staff of the forestry administration of Changsha County, Hunan Province, for their support.

Author contributions

All authors contributed to this manuscript: research idea and study design: XF; data collection and analyses: XG, XF, SZ, and LP, with support from WX, CP and YK; manuscript writing: XG, YZ, WX, and CP.

References

Ajami, M., Heidari, A., Khormali, F., Gorji, M., Ayoubi, S., 2016. Environmental factors controlling soil organic carbon storage in loess soils of a subhumid region, northern Iran. Geoderma 281, 1–10.
An, S.S., Mentler, A., Mayer, H., Blum, W.E.H., 2010. Soil aggregation, aggregate stability, organic carbon and nitrogen in different soil aggregate fractions under forest and shrub vegetation on the Loess Plateau, China. Catena 81, 226–233.
Arthur, M.A., Fahey, T.J., 1992. Biomass and nutrients in an Engelmann spruce-subalpine fir forest in north central Colorado: pool, annual production and internal cycling. Can. J. For. Res. 22, 315–325.
Barreto, P.A.B., Gama-Rodrigues, E.F., Gama-Rodrigues, A.C., Fontes, A.G., Polidoro, J.C., Moço, M.K.S., Machado, R.C.R., Baligar, V.C., 2011. Distribution of oxidizable organic C fractions in soils under cacao agroforestry systems in Southern Bahia, Brazil. Agrofor. Syst. 81, 213–220.
Chabbi, A., KÖgelknabner, I., Rumpel, C., 2009. Stabilised carbon in subsoil horizons is located in spatially distinct parts of the soil profile. Soil Biol. Biochem. 41, 256–261.
Chen, C.R., Xu, Z.H., Mathers, N.J., 2004. Soil carbon pools in adjacent natural and plantation forests of subtropical Australia. Soil Sci. Soc. Am. J. 68, 282–291.
Chen, G.C., Gao, M., Pang, B.P., Chen, S.Y., Ye, Y., 2018. Top-meter soil organic carbon stocks and sources in restored mangrove forests of different ages. For. Ecol. Manag. 422, 87–94.
Cochran, R.L., Collins, H.P., Kennedy, A., Bezdicek, D.F., 2007. Soil carbon pools and fluxes after land conversion in a semiarid shrub-steppe ecosystem. Biol. Fertil. Soils 43, 479–489.
Crow, S.E., Lajtha, K., Bowden, R.D., Yano, Y., Brant, J.B., Caldwell, B.A., Sulzman, E.W., 2009. Increased coniferous needle inputs accelerate decomposition of soil carbon in an old-growth forest. For. Ecol. Manag. 258, 2224–2232.
Deng, L., Wang, K.B., Chen, M.L., Shangguan, Z.P., Sweeney, S., 2013. Soil organic carbon storage capacity positively related to forest succession on the Loess Plateau, China. Catena 110, 1–7.
Deng, L., Wang, K.B., Tang, Z.S., Shangguan, Z.P., 2016. Soil organic carbon dynamics following natural vegetation restoration: evidence from stable carbon isotopes (δ13C). Agric. Ecosyst. Environ. 221, 235–244.
Dikgwatlhe, S.B., Kong, F.L., Chen, Z.D., Lal, R., Zhang, H.L., Chen, F., 2014. Tillage and residue management effects on temporal changes in soil organic carbon and fractions of a silty loam soil in the North China Plain. Soil Use Manag. 30, 496–506.
Fortuna, A., Harwood, R.R., Paul, E.A., 2003. The effects of compost and crop rotations on carbon turnover and the particulate organic matter fraction. Soil Sci. 168, 434–444.
Francaviglia, R., Renzi, G., Ledda, L., Benedetti, A., 2017. Organic carbon pools and soil biological fertility are affected by land use intensity in Mediterranean ecosystems of Sardinia, Italy. Sci. Total Environ. 599-600, 789–796.
García-Díaz, A., Marqués, M.J., Sastre, B., Bienes, R., 2018. Labile and stable soil organic carbon and physical improvements using groundcovers in vineyards from central Spain. Sci. Total Environ. 621, 387–397.
Hyvönen, R., Agren, G.I., Linder, S., Persson, T., Cotrufo, M.F., Ekblad, A., Freeman, M., Grelle, A., Janssens, I.A., Jarvis, P.G., Kellomaki, S., Lindroth, A., Loustau, D., Lundmark, T., Norby, R.J., Oren, R., Pilegaard, K., Ryan, M.G., Sigurdsson, B.D., Stromgren, M., van Oijen, M., Wallin, G., 2007. The likely impact of elevated CO_2, nitrogen deposition, increased temperature and management on carbon sequestration in temperate and boreal forest ecosystems: a literature review. New Phytol. 173, 463–480.
Iqbal, J., Hu, R.G., Lin, S., Ahamadou, B., Feng, M.L., 2009. Carbon dioxide emissions from Ultisol under different land uses in mid–subtropical China. Geoderma 152, 63–73.
IUSS (International Union of Soil Sciences) Working Group WRB, 2006. World Reference Base for Soil Resource 2006. World Soil Resources Reports No. 103 FAO, Rome.
Jha, P., De, A., Lakaria, B.L., Biswas, A.K., Singh, M., Reddy, K.S., Rao, A.S., 2012. Soil carbon pools, mineralization and fluxes associated with land use change in vertisols of Central India. Natl. Acad. Sci. Lett. 35, 475–483.
Kemmitt, S.J., Wright, D., Goulding, K.W.T., Jones, D.L., 2006. pH regulation of carbon and nitrogen dynamics in two agricultural soils. Soil Bio. Biochem. 38, 898–911.
Kirkby, C.A., Kirkegaard, J.A., Richardson, A.E., Wade, L.J., Blanchard, C., Batten, G., 2011. Stable soil organic matter: a comparison of C:N:P:S ratios in Australian and other world soils. Geoderma 163, 197–208.
Li, D.H., Gao, G.Y., Lü, Y.H., Fu, B.J., 2016a. Multi-scale variability of soil carbon and nitrogen in the middle reaches of the Heihe River basin, northwestern China. Catena 137, 328–339.
Li, Q., Chen, D.D., Zhao, L., Yang, X., Xu, S.X., Zhao, X.Q., 2016b. More than a century of Grain for Green Program is expected to restore soil carbon stock on alpine grassland revealed by field 13C pulse labeling. Sci. Total Environ. 550, 17–26.
Li, Z., Liu, C., Dong, Y., Chang, X., Nie, X., Liu, L., Xiao, H., Lu, Y., Zeng, G., 2017. Response of soil organic carbon and nitrogen stocks to soil erosion and land use types in the Loess hilly-gully region of China. Soil Tillage Res. 166, 1–9.
Lian, Z.L., Jiang, Z.J., Huang, X.P., Liu, S.L., Zhang, J.P., Wu, Y.C., 2018. Labile and recalcitrant sediment organic carbon pools in the Pearl River Estuary, southern China. Sci. Total Environ. 640–641, 1302–1311.

Liu, C., Xiang, W.H., Lei, P.F., Deng, X.W., Tian, D.L., Fang, X., Peng, C.H., 2014. Standing fine root mass and production in four Chinese subtropical forests along a succession and species diversity gradient. Plant Soil 376, 445–459.
Liu, S.J., Zhang, W., Wang, K., Pan, F.J., Yang, S., Shu, S.Y., 2015. Factors controlling accumulation of soil organic carbon along vegetation succession in a typical karst region in Southwest China. Sci. Total Environ. 521-522, 52–58.
Liu, X., Li, L., Qi, Z., Han, J., Zhu, Y., 2017. Land-use impacts on profile distribution of labile and recalcitrant carbon in the ili river valley, northwest China. Sci. Total Environ. 586, 1038–1045.
von Lützow, M.V., Kögel-Knabner, I., Ekschmitt, K., Flessa, H., Guggenberger, G., Matzner, E., Marschner, B., 2007. SOM fractionation methods: relevance to functional pools and to stabilization mechanisms. Soil Biol. Biochem. 39, 2183–2207.
Madonsela, S., Cho, M.A., Ramoelo, A., Mutanga, O., Naidoo, L., 2018. Estimating tree species diversity in the savannah using NDVI and woody canopy cover. Int. J. Appl. Earth Obs. Geoinformation 66, 106–115.
Marchand, C., 2017. Soil carbon stocks and burial rates along a mangrove forest chronosequence (French Guiana). For. Ecol. Manag. 384, 92–99.
Nath, A.J., Brahma, B., Sileshi, G.W., Das, A.K., 2018. Impact of land use changes on the storage of soil organic carbon in active and recalcitrant pools in a humid tropical region of India. Sci. Total Environ. 624, 908–917.
Pandey, D., Agrawal, M., Bohra, J.S., Adhya, T.K., Bhattacharyya, P., 2014. Recalcitrant and labile carbon pools in a sub-humid tropical soil under different tillage combinations: a case study of rice-wheat system. Soil Tillage Res. 143, 116–122.
Paul, E.A., Harris, D., Collins, H.P., Schulthess, U., Robertson, G.P., 1999. Evolution of CO_2 and soil carbon dynamics in biologically managed, row-crop agroecosystems. Appl. Soil Ecol. 11, 53–65.
Paul, E.A., Collins, H.P., Leavitt, S.W., 2001. Dynamics of resistant soil carbon of Midwestern agricultural soils measured by naturally occurring ^{14}C abundance. Geoderma 104, 239–256.
Paul, E.A., Morris, S.J., Conant, R.T., Plante, A.F., 2006. Does the acid hydrolysis-incubation method measure meaningful soil organic carbon pools? Soil Sci. Soc. Am. J. 70, 1023–1035.
Powers, J.S., Marín-Spiotta, E., 2017. Ecosystem processes and biogeochemical cycles in secondary tropical forest succession. Annu. Rev. Ecol. Evol. Syst. 48, 497–519.
Qian, H.Y., Pan, J.J., Sun, B., 2013. The relative impact of land use and soil properties on sizes and turnover rates of soil organic carbon pools in Subtropical China. Soil Use Manag. 29, 510–518.
R Core Team, 2015. R: A Language and Environment for Statistical Computing. R Foundation for Statistical Computing, Vienna, Austria URL. https://www.r-project.org/.
Ramesh, T., Manjaiah, K.M., Mohopatra, K.P., Rajasekar, K., Ngachan, S.V., 2015. Assessment of soil organic carbon stocks and fractions under different agroforestry systems in subtropical hill agroecosystems of north-east India. Agrofor. Syst. 89, 677–690.
Rasse, D.P., Rumpel, C., Dignac, M.F., 2005. Is soil carbon mostly root carbon? Mechanisms for a specific stabilisation. Plant Soil 269, 341–356.
Richter, D.D., Markewitz, D., Trumbore, S.E., Wells, C.G., 1999. Rapid accumulation and turnover of soil carbon in a re-establishing forest. Nature 400, 56–58.
Robertson, A.I., Alongi, D.M., 2016. Massive turnover rates of fine root detrital carbon in tropical Australian mangroves. Oecologia 180, 841–851.
Rosell, R.A., Galantini, J.A., Suñer, L.G., 2000. Long-term crop rotation effects on organic carbon, nitrogen, and phosphorus in Haplustoll soil fractions. Arid Soil Res. Rehab. 14, 309–315.
Rovira, P., Vallejo, V.R., 2007. Labile, recalcitrant, and inert organic matter in Mediterranean forest soils. Soil Biol. Biochem. 39, 202–215.
Russell, A.E., Cambardella, C.A., Ewel, J.J., Parkin, T.B., 2004. Species, rotation, and life-form diversity effects on soil carbon in experimental tropical ecosystems. Ecol. Appl. 14, 47–60.
Sá, J.C.D.M., Lal, R., 2009. Stratification ratio of soil organic matter pools as an indicator of carbon sequestration in a tillage chronosequence on a Brazilian Oxisol. Soil Tillage Res. 103, 46–56.
Schimel, J.P., Weintraub, M.N., 2003. The implications of exoenzyme activity on microbial carbon and nitrogen limitation in soil: a theoretical model. Soil Biol. Biochem. 35, 549–563.
Six, J., Conant, R.T., Paul, E.A., Paustian, K., 2002. Stabilization mechanisms of soil organic matter: implications for C-saturation of soils. Plant Soil 241, 155–176.
Smith, W.N., Grant, B.B., Campbell, C.A., Mcconkey, B.G., Desjardins, R.L., Kröbel, R., Malhi, S.S., 2012. Crop residue removal effects on soil carbon: measured and inter-model comparisons. Agric. Ecosyst. Environ. 161, 27–38.
Song, X.Z., Kimberley, M.O., Zhou, G.M., Wang, H.L., 2017. Soil carbon dynamics in successional and plantation forests in subtropical China. J. Soils Sediments 17, 2250–2256.
Sun, Z.Y., Ren, H., Schaefer, V., Guo, Q.F., Wang, J., 2014. Using ecological memory as an indicator to monitor the ecological restoration of four forest plantations in subtropical China. Environ. Monit. Assess. 186, 8229–8247.
Tang, C.Q., Zhao, M.H., Li, X.S., Ohsawaet, M., Ou, X.K., 2010a. Secondary succession of plant communities in a subtropical mountainous region of SW China. Ecol. Res. 25, 149–161.
Tang, J.W., Cao, M., Zhang, J.H., Li, M.H., 2010b. Litterfall production, decomposition and nutrient use efficiency varies with tropical forest types in Xishuangbanna, SW China: a 10-year study. Plant Soil 335, 271–288.
Tian, Q., He, H., Cheng, W., Zhen, B., Yang, W., Zhang, X., 2016. Factors controlling soil organic carbon stability along a temperate forest altitudinal gradient. Sci. Rep. 6, 1–9.
Wang, H., Liu, S.R., Wang, J.X., Shi, Z.M., Xu, J., Hong, P.Z., Ming, A.G., Yu, H.L., Chen, L., Lu, L.H., Cai, D.X., 2016. Differential effects of conifer and broadleaf litter inputs on soil organic carbon chemical composition through altered soil microbial community composition. Sci. Rep. 6, 1–9.
Wang, Y.X., Ran, L.S., Fang, N.F., Shi, Z.H., 2018. Aggregate stability and associated organic carbon and nitrogen as affected by soil erosion and vegetation rehabilitation on the Loess Plateau. Catena 167, 257–265.
West, T.O., Six, J., 2007. Considering the influence of sequestration duration and carbon saturation on estimates of soil carbon capacity. Clim. Chang. 80, 25–41.
Wiesmeier, M., Schad, P., von Lützow, M., Poeplau, C., Spörlein, P., Geuß, U., Hangen, E., Reischl, A., Schilling, B., Kögel-Knabner, I., 2014. Quantification of functional soil organic carbon pools for major soil units and land uses in southeast Germany (Bavaria). Agri. Ecosyst. Environ. 185, 208–220.
Xiang, W.H., Fang, X., 2018. Structure and Soil Properties in Subtropical Secondary Forests. Science Press, Beijing (in Chinese).
Xiang, X.H., Liu, S.H., Lei, X.D., Frank, S.C., Tian, D.L., Wang, G.J., Deng, X.W., 2013. Secondary forest floristic composition, structure, and spatial pattern in subtropical China. J. For. Res. 18, 111–120.
Xiang, W.H., Zhou, J., Ouyang, S., Zhang, S.L., Lei, P.F., Li, J.X., Deng, X.W., Fang, X., Forrester, D.I., 2016. Species-specific and general allometric equations for estimating tree biomass components of subtropical forests in southern China. Eur. J. For. Res. 135, 1–17.
Xiao, Y.H., Tong, F.C., Liu, S.R., Kuang, Y.W., Chen, B.F., Huang, J.B., 2016. Response of soil labile organic carbon fractions to forest conversions in subtropical China. Trop. Ecol. 57, 691–699.
Xie, J.S., Guo, J.F., Yang, Z.J., Huang, Z.Q., Chen, G.S., Yang, Y.S., 2013. Rapid accumulation of carbon on severely eroded red soils through afforestation in subtropical China. For. Ecol. Manag. 300, 53–59.
Yang, L., Pan, J., Shao, Y., Chen, J.M., Ju, W.M., Shi, X., Yuan, S., 2007. Soil organic carbon decomposition and carbon pools in temperate and sub-tropical forests in China. J. Environ. Manag. 85, 690–695.
Yang, Y.S., Guo, J., Chen, G.S., Yin, Y.F., Gao, R., Lin, C.F., 2009. Effects of forest conversion on soil labile organic carbon fractions and aggregate stability in subtropical China. Plant Soil 232, 153–162.
Yang, T., Adams, J.M., Shi, Y., He, J.S., Jing, X., Chen, L.T., Tedersoo, L., Chu, H.Y., 2017. Soil fungal diversity in natural grasslands of the Tibetan Plateau: associations with plant diversity and productivity. New Phytol. 215, 756–765.
Yu, P.J., Han, K.X., Li, Q., Zhou, D.W., 2017. Soil organic carbon fractions are affected by different land uses in an agro-pastoral transitional zone in northeastern China. Ecol. Indic. 73, 331–337.
Zhang, H., Zhou, Z., 2018. Recalcitrant carbon controls the magnitude of soil organic matter mineralization in temperate forests of northern China. For. Ecosyst. 3, 211–220.
Zhang, J., Wang, S.L., Feng, Z.W., Wang, Q.K., 2009. Stability of soil organic carbon changes in successive rotations of Chinese fir (*Cunninghamia lanceolata* (Lamb.) Hook) plantations. J. Environ. Sci. 21, 352–359.
Zhao, Y.G., Liu, X.F., Wang, Z.L., Zhao, S.W., 2015. Soil organic carbon fractions and sequestration across a 150-yr secondary forest chronosequence on the Loess Plateau, China. Catena 133, 303–308.
Zhou, G.Y., Zhou, C.Y., Liu, S.G., Tang, X.L., Ouyang, X.J., Zhang, D.Q., Liu, S.Z., Liu, J.X., Yan, J.H., Zhou, C.H., Luo, Y., Guan, L.L., Liu, Y., 2006. Belowground carbon balance and carbon accumulation rate in the successional series of monsoon evergreen broad-leaved forest. Science in China (Series D) 49, 311–332.
Zhu, Z.K., Zeng, G.J., Ge, T.D., Hu, Y.J., Tong, C.L., Shibistova, O., He, X.H., Wang, J., Guggenberger, G., Wu, J.S., 2016. Fate of rice shoot and root residues, rhizodeposits, and microbe-assimilated carbon in paddy soil - Part 1: Decomposition and priming effect. Biogeosciences 13, 4481–4489.
Zhu, Z.K., Ge, T.D., Hu, Y.J., Zhou, P., Wang, T.T, Shibistova, O., Guggenberger, G., Su, Y.R., Wu, J.S., 2017. Fate of rice shoot and root residues, rhizodeposits, and microbial assimilated carbon in paddy soil - part 2: turnover and microbial utilization. Plant and Soil 416, 243–257.